

# Development & Testing of a Reliability Performance Index for Modular Robotic Systems

Dean L. Schneider • Air Force Institute of Technology • Wright-Patterson AFB

Delbert Tesar • University of Texas at Austin • Austin

J. Wesley Barnes • University of Texas at Austin • Austin

Key Words: Modular Robotic Systems, Reliability Index, Kinematic Reliability, Accuracy

DTIC  
DIRECT  
NOV 01 1993  
A D

This document has been approved  
for public release and sale; its  
distribution is unlimited.

## SUMMARY AND CONCLUSIONS

Several research groups across the country are interested in the development of modular robotics systems. One issue pertaining to modular robotic systems is the integration of modules into a fully functional robot system. Two criteria for modules integration not previously investigated are the reliability and accuracy of the system. This paper presents the results of the development of a framework for a "criterion" embodying these two modular robot characteristics.

Using a probabilistic representation of manipulator kinematics and a reliability block diagram model of the manipulator system, a Reliability Performance Index (RPI) representing the probability of no hardware or software failure and the manipulator achieving a specified position and orientation is developed. The RPI is tested with a case study consisting of a three degree-of-freedom planar manipulator assembled from a choice of six joint modules of varying reliability and precision and a choice of six link module combinations of varying lengths and machining tolerances. A straight-line, square trajectory is specified and the RPI is calculated for each combination of joint modules and links, a total of 1296 different combinations. An Analysis of Variance (ANOVA) is performed on the results using the different joint locations and link options as factors and the different joint modules and link options as factor levels. The different factors are tested for significance and the Tukey Studentized Range Test is performed to determine significance of the different joint modules and link options.

Using this statistical testing, a 70% reduction in the module design space is achieved using the RPI. Optimization using other appropriate manipulator criteria can then be performed to generate the final configuration. Additional extensive case studies are needed to fully develop the RPI to a stage necessary for implementation into a computer-aided design system for modular robot configuration design. The RPI may also be useful in the quantification of the overall system reliability and performance of any system based upon measured error, such as control systems.

## 1. INTRODUCTION

Several concepts of modular robotic systems have been presented and developed over the past several years. For practical operation, the system will need to be configured for a particular application or task from a suite of available modules. This integration requires the use of different criteria on which to base the module selection. One of these criteria is the accuracy of the robotic system. Another criterion is the reliability of the system. In several applications, both of these criteria are the over-riding characteristics, including microelectronics assembly [11], space applications [3] and nuclear reactor maintenance [10]. This paper presents a framework for the formulation of a reliability index, quantifying the statistical characteristics of modular robot system reliability and accuracy.

*Nomenclature and Notation.* The notation used in this paper follows standard statistical practice with the meanings of various terms defined as they are used.

## 2. RELIABILITY PERFORMANCE INDEX FORMULATION

For a robotic system, failure can be defined as the manipulator not reaching a commanded position and orientation (denoted together as the "pose" of the robot) within a certain error bound. There are two basic causes for this failure: variation in the kinematic parameters of the robotic system, and/or a failure in the hardware or software of the system causing the robot not to achieve the commanded pose. If we can assume that these two causes of failure are *s*-independent (which can be justified except in those cases of a fault-tolerant manipulator where a hardware failure does not cause a failure of the system to achieve a pose), we can form a Reliability Performance Index (RPI) using a serial combination of the hardware, software, and kinematic reliability functions of the manipulator. In its most general formulation the RPI can be expressed as

$$RPI(t) = R_h(t) \cdot R_s(t) \cdot R_k(t) \quad (1)$$

93-26265



93 10 20 044

where  $R_h(t)$  = the system hardware reliability function  
 $R_s(t)$  = the system software reliability function  
 $R_k(t)$  = the system kinematic reliability function

If the  $s$ -independence assumption is satisfied, the RPI is the probability that the manipulator will move to the commanded pose. The time dependence of Equation (1) allows for the future development of a dynamic criterion but due to the current limitations in robot system metrology, we cannot as yet quantify a time based degradation in the kinematic reliability function as it is developed in the next section. For this reason, a simpler, static formulation of the RPI is made as

$$RPI = R_h \cdot R_s \cdot R_k \quad (2)$$

The derivation of the kinematic reliability model follows.

### 3. KINEMATIC RELIABILITY

The static kinematic reliability represents the probability of the pose of the manipulator end-effector being within a certain error bound due to kinematic variations. This concept was first proposed by Bhatti and Rao [2]. The kinematic reliability is a direct indicator of the accuracy of the manipulator and is based upon the sources of error in the manipulator kinematics. These errors can be caused by compliances, machining tolerances, position measurements etc. and can be represented as variations in the kinematic variables of a robotic system. As a first step, these kinematic variables are assumed to be  $s$ -normally distributed.

The kinematics of a manipulator can be expressed via the Denavit-Hartenberg (D-H) formulation [5]. In the D-H notation, two parameters are associated with each link ( $a_i$  and  $\alpha_i$ ) and two with each joint ( $d_i$  and  $\theta_i$ ). The distance  $d_i$  and the angle  $\theta_i$  between adjacent links give the relative position between the links and the length  $a_i$  and twist angle  $\alpha_i$  determine the structure of the link. For revolute joints,  $d_i$ ,  $a_i$ , and  $\alpha_i$  are the structural parameters and  $\theta_i$  is the joint variable. For prismatic joints,  $\theta_i$  is a structural parameter and  $d_i$  is the joint variable.

The direct kinematic problem is to solve for the position and orientation of the end-effector given the arm structural parameters and the values of the joint variables. Coordinate frames are attached to each link and transformation matrices from link frame to link frame are written in terms of the relevant kinematic and joint parameters. This transformation relating link frame  $i$  to link frame  $i-1$  (known as the D-H transformation matrix) can be shown to be

$$[A_{i-1}^i] = \begin{bmatrix} C\theta_i & -C\alpha_i S\theta_i & S\alpha_i S\theta_i & a_i C\theta_i \\ S\theta_i & C\alpha_i C\theta_i & -S\alpha_i C\theta_i & a_i S\theta_i \\ 0 & S\alpha_i & C\alpha_i & d_i \\ 0 & 0 & 0 & 1 \end{bmatrix} \quad (3)$$

where C denotes cosine and S denotes sine [4]. Using this notation, the end-effector position and orientation can be calculated as

$$[T] = [A_0^1][A_1^2] \cdots [A_{n-1}^n] = \prod_{i=1}^n [A_{i-1}^i] \quad (4)$$

where  $n$  denotes the number of joints in the manipulator system.  $[T]$  is called the arm matrix. The end-effector position is found from the right-most column vector of the arm matrix. The upper-left 3 by 3 partition is the rotation matrix from the base frame to the end-effector frame.

We can now define the kinematic reliability of the manipulator to be the probability of the end-effector being in a certain pose within a specified error bound due to errors in the kinematic variables. This implies the definition of a permissive region about the desired end-effector position. Using Bhatti and Rao's notation, we choose to use the Type III permissive region which is a box or sphere shaped region about the desired position. The box shaped positional kinematic reliability of the manipulator can be described as

$$R_{KIII} = P\{(x_d - \Delta x < x^* < x_d + \Delta x) \cup (y_d - \Delta y < y^* < y_d + \Delta y) \cup (z_d - \Delta z < z^* < z_d + \Delta z)\} \quad (5)$$

where  $(x_d, y_d, z_d)$  is the desired end-effector position and  $(\Delta x, \Delta y, \Delta z)$  is the specified tolerance on the position. A similar definition can be made for the spherical permissive region.

Two methods can be used to determine the kinematic reliability for a manipulator. The analytical method uses the algebra of random variables to determine the end-effector position and orientation  $s$ -probability distribution function and then integrates over the permissive region to determine the kinematic reliability. This approach is mathematically intractable since a general manipulator will require a  $s$ -hexivariate distribution to describe the pose of the manipulator.

An alternative to this approach is to use Monte Carlo simulation to determine the kinematic reliability. A  $s$ -probability distribution of each kinematic variable is determined or assumed and a sample is taken from each of these distributions is taken. These samples are then substituted into Equation (4) and the end-effector position and orientation for those samples are determined. This pose is a sample from the end-effector position and orientation  $s$ -distribution [12]. This sample can be compared to the permissive region and if it is inside, the trial is considered a success. The kinematic reliability is then the ratio of the number of successes to the total number of trials as expressed in Equation (6).

$$R_k = \frac{\text{number of successful trials}}{\text{total number of trials}} \quad (6)$$

One problem encountered at this point is the fact that the accuracy and repeatability, and thus the kinematic

A-1

reliability, varies over the workspace [13]. If we are to use the formulation of Equation (2), we need to have a single value of  $R_k$  over the workspace or trajectory. Based on computational issues, we chose to use the minimum value of the kinematic reliability over the workspace or specified trajectory. This also provides the most conservative index value.

### 3. HARDWARE AND SOFTWARE RELIABILITY

The other component of the RPI needed for Equation (2) is a quantification of the hardware and software reliability. The different types of hardware reliability models considered where reliability block diagrams [7], Markov models [15], and Fault Tree models [6]. The software models considered were two modular models, the Littlewood model [9] and the Kubat model [8]. The criteria used to select the models were modularity of the model, modularity of the data required for the model, computational complexity, and the ability to include fault tolerance in the model at a later date.

Based on rankings for each model in each category, the reliability block diagram model was selected for the hardware reliability model and the Littlewood modular software reliability model was chosen. For most robotic systems, the hardware reliability structure is serial since the failure of one component will cause the failure of the system. The hardware component of the RPI can be expressed as

$$R_h(t) = \prod_{i=1}^n R_i(t) \quad (7)$$

where  $n$  is the number of modules and  $R_i(t)$  is the reliability function for the  $i$ th module.

The Littlewood modular software model is an  $s$ -exponential failure model and the  $s$ -failure rate can be represented as

$$\lambda_{s/w} = \sum_i a_i v_i + \sum_{ij} b_{ij} \lambda_{ij} \quad (8)$$

where  $a_i$  = the proportion of time spent in module  $i$ ,  
 $b_{ij}$  = the frequency of transfer of control from module  $i$  to module  $j$ ,  
 $v_i$  = software module  $i$  failure rate, and  
 $\lambda_{ij}$  = the probability of failure during control transfer from  $i$  to  $j$ .

The hardware and software models are time-dependent, so we must choose a time of evaluation to obtain a static value to use in Equation (2). Since the RPI is meant to be a comparative tool, a single time of evaluation for all the modules will provide a relative number on which to base the comparisons. We chose to evaluate the time as

$$t \leq \frac{1}{2} \theta_{Min} \quad (9)$$

where  $\theta_{Min}$  is the minimum expected life of any hardware or software module in the system.

To demonstrate the utility of the RPI and how it is calculated, a limited case study is presented next.

### 4. RPI EXAMPLE

#### 4.1. The Manipulator

The objective of this example is to use the RPI to help select the modules from a suite of available modules. The desired system is a 3 Degree-Of-Freedom (DOF) manipulator shown in Figure 1. This manipulator is expected to perform the trajectory illustrated in Figure 2. The position tolerance is  $\pm 0.001$  meter in both  $x$  and  $y$  directions and  $0.1^\circ$  on the orientation of the end-effector. The available components are listed in Tables 1 and 2. The links are assumed to have a zero failure rate and the joint modules are assumed to have a constant failure rate that is proportional to the precision (inversely proportional to the standard deviation of the joint module position). Each link combination represents a different inverse kinematic solution. The inverse kinematics for each link option was derived after Craig [4] and the required joint angles to achieve each position annotated in Figure 2 where calculated. The kinematics of the system of Figure 1 are

$$\begin{aligned} x &= l_1 \cos \theta_1 + l_2 \cos(\theta_1 + \theta_2) \\ y &= l_1 \sin \theta_1 + l_2 \sin(\theta_1 + \theta_2) \\ \Phi &= \theta_1 + \theta_2 + \theta_3 \end{aligned} \quad (10)$$

where  $x$  and  $y$  represent the end-effector position and  $\Phi$  represents the end-effector orientation. Using a rectangular permissive region and an angular tolerance on the end-effector orientation, we can represent the kinematic reliability of the system as

$$R_k(x, y, \Phi) = P \left\{ \begin{aligned} &(x_d - 0.001 \leq x \leq x_d + 0.001) \cup \\ &(y_d - 0.001 \leq y \leq y_d + 0.001) \cup \\ &(\Phi_d - 0.1 \leq \Phi \leq \Phi_d + 0.1) \end{aligned} \right\} \quad (11)$$

and

$$R_k = \min R_k(x, y, \Phi) \quad (12)$$

The hardware reliability of the system is assumed exponential and can be expressed as

$$R_h(t) = e^{-\lambda_s t} \quad (13)$$

where

$$\lambda_s = \lambda_{Base} + \lambda_{Elbow} + \lambda_{Wrist} \quad (14)$$

since the links do not contribute to the system failure rate. Equation (14) does not include the controller or software that would be necessary to control this system which makes  $R_s = 1$  in Equation (2), although these components can be easily added if data is available. Examining Table 2, it is seen that the minimum Mean-Time-Between-Failure (MTBF)

( = inverse of the failure rate) for the joint modules is 1852 hours (module 6). The time chosen for hardware reliability evaluation is 100 hours, which satisfies the suggested criterion of Equation (9).

A Monte Carlo simulation is performed to evaluate the kinematic reliability of the system at each position of the trajectory of Figure 2 for each link option and joint module combination. Five hundred trials at each end-effector position are generated and the kinematic reliability at that position is calculated with Equation (6). The minimum kinematic reliability over the workspace is used to represent the system kinematic reliability per Equation (13). Each simulation was repeated five times and the results were averaged to obtain the system kinematic reliability for the particular link and actuator combination. The hardware reliability was evaluated per Equation (13) for each combination of joint modules and the RPI was calculated per Equation (2).

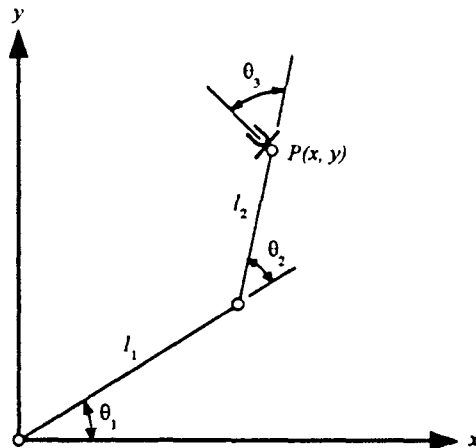


Figure 1. Three Degree of Freedom Manipulator

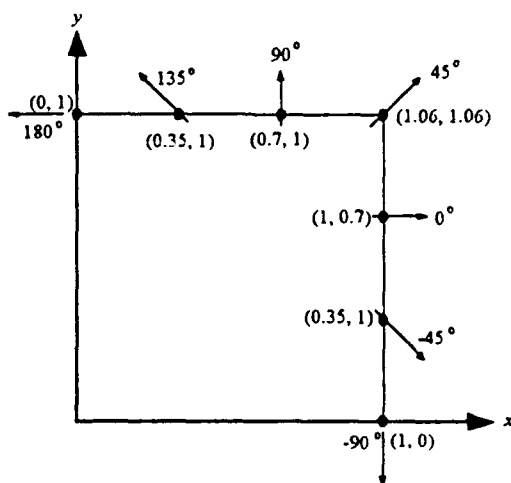


Figure 2. Rectangular Motion Path for the 3-DOF Manipulator (Arrow Indicates End-Effector Orientation)

Table 1. Link Module Characteristics

| Option | $l_1$ (m) | $l_2$ (m) | $\lambda/10^6$ hr | $\sigma$ (m) |
|--------|-----------|-----------|-------------------|--------------|
| 1      | 0.75      | 0.75      | 0.0               | 0.0001       |
| 2      | 1.0       | 0.5       | 0.0               | 0.0001       |
| 3      | 0.5       | 1.0       | 0.0               | 0.0001       |
| 4      | 0.75      | 0.75      | 0.0               | 0.001        |
| 5      | 1.0       | 0.5       | 0.0               | 0.001        |
| 6      | 0.5       | 1.0       | 0.0               | 0.001        |

Table 2. Actuator Module Characteristics

| Joint Module # | $\lambda$ (/10 <sup>6</sup> hours) | $\sigma$ (degrees) |
|----------------|------------------------------------|--------------------|
| 1              | 40                                 | 0.1                |
| 2              | 140                                | 0.05               |
| 3              | 240                                | 0.01               |
| 4              | 340                                | 0.005              |
| 5              | 440                                | 0.001              |
| 6              | 540                                | 0.0005             |

#### 4.2 Optimization and Design Selection

Figure 3 shows a history of how the RPI changes as the joint modules are changed for link option 1. The horizontal axis is the joint module combination. Joint module combination 1 corresponds to the joint module one in each joint location (Base, Elbow, Wrist) = (1, 1, 1) and combination 216 corresponds to joint module 6 in each location (6, 6, 6). The simulations iterated from the wrist inward, making joint modular combination 2 represent the joint module locations (1, 1, 2). This history was repeated for each of the six link module combinations tested in Table 1. Figure 3 is representative of the higher tolerance (smaller variance) links. Figure 4 shows the same behavior but with lower RPI values for the lower tolerance (higher variance) links.

The first question to be examined is "does the maximum RPI value correspond to a maximum in the design space and does this represent an optimum point in the design space?" We first must describe what we mean by "optimum." In the

context of the RPI, we are searching for the combination of actuators that will maximize both system reliability and accuracy (as represented by the kinematic reliability). Usually, the optimization objective function is a function of the design variables. However, in the case of the RPI, the design variables are not explicit and we must address what the maximum actually means.

The RPI basic formulation is found in Equation (2). All components, the hardware reliability and the kinematic reliability, are measures of probability and are bounded to be non-negative and less than or equal to unity, thus the maximum value of the RPI is unity representing a certainty of no failures as well as always being inside the permissible pose region. The highest value of kinematic reliability means that the particular combination is the most accurate, having the highest probability of being inside the error bound on the pose. The highest value of hardware reliability means that the particular combination of components is the most reliable of all the combinations. One might decide to pick the most accurate combination that has a reliability of at least, say, 0.98 at 100 hours or the objective may be reversed: the highest reliability with at least a 0.9 kinematic reliability.

Table 3 presents the results of the simulations of the trajectory of Figure 2. A large difference can be seen between the maximum and minimum values for the different link and joint module combinations. The most immediate difference can be seen between the two sets of tolerances of the link modules. The higher tolerance links make a tremendous difference in the value of the achieved RPI. Based upon the maximum value of the RPI of unity, one would select link option 2 with joint module #3 in every joint position. This is the deterministic approach. However, the maximum RPI values are extremely close together, within one standard deviation of the mean RPI. The statistical significance of this fact is discussed next.

Additional deterministic numerical optimizations were performed on the hardware and kinematic reliabilities using the other component of the RPI as a constraint. Conceptually, these optimizations can be performed analytically if the hardware and kinematic reliabilities can be expressed analytically. However, since the case study example is empirical, only empirical optimizations were made. One aspect of this particular exercise must be noted:  $R_k$  is a stochastic variable with a standard deviation. In general, the failure rates of Tables 1 and 2 will be estimates based on test data having their own means and variances. In this particular case,  $R_h$  is considered a constant (since it was evaluated from an assumed known distribution) and the only variability in the value of the RPI comes from the kinematic reliability although this would not be true in a general case. This variability prevents a deterministic optimization from providing an accurate answer, since the variation can cause the optimum to vary widely over the design space. However, performing a deterministic optimization using the values of  $R_k$  at this stage is useful to observe the general tendencies of the behavior of the RPI when compared to its components.

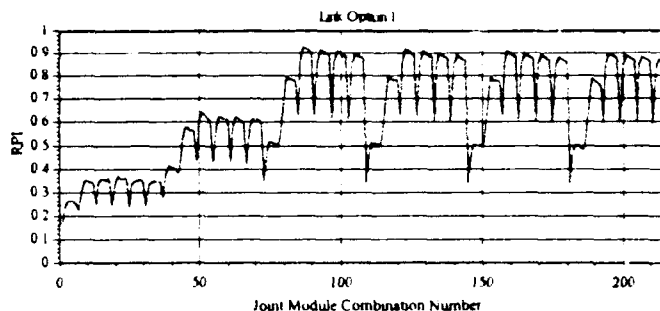


Figure 3. RPI by Joint Module Combinations: Link Option 1,  $l_1 = l_2 = 0.75$  m, Tolerance = 0.0001 m

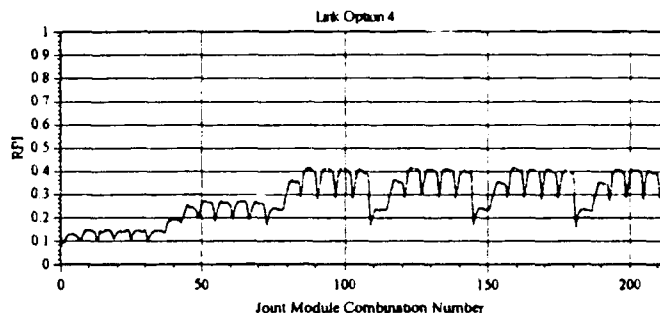


Figure 4. RPI by Joint Module Combinations: Link Option 4,  $l_1 = l_2 = 0.75$  m, Tolerance = 0.001 m

All of these optimizations provided maximums and minimums very close to the same maximum and minimum points (expressed as joint combinations) as the numerical results of Table 3, with the difference in the values results from the variation in the kinematic reliability. This limited data example indicates that the RPI has a tendency to the same maximum that a deterministic optimization on both RPI components will find. While not a one-to-one correlation on maximum points, the optimum configurations are very close in their characteristics, indicating "adjacent" points. This indicates confidence can be placed in the RPI to identify a configuration that possesses a satisfactory trade-off between precision and system reliability.

If we examine the plots of the RPI vs. the joint module combinations in Figures 3 and 4, we see a definite difference between the different joint modules and the locations they are in. The most obvious aspect is having joint module 1 (highest hardware reliability and lowest tolerance) and joint module 2 have much lower values of the RPI no matter what modules are in the distal locations. The deep dips are also due to the use of joint modules 1 and 2 in the distal locations. The standard deviations of the joint modules also have a significant impact. Figures 3 and 4 give a clear indication of when the kinematic reliability component of the RPI dominates the hardware reliability. For standard deviations of the joint modules greater than or equal to  $\sigma_0 = 0.05$ , the RPI is dominated by the lack of accuracy in the modules. When the standard deviations are less than 0.05, the system is accurate enough and the hardware reliability becomes important.

**Table 3. Maximum and Minimum Results from RPI Simulation of Figure 2.**

| Link Opt | B | E | w | Min/Max | $R_h$   | $R_k$   | RPI     |
|----------|---|---|---|---------|---------|---------|---------|
| 1        | 3 | 3 | 3 | Max     | 0.93044 | 0.99987 | 0.93034 |
|          | 1 | 1 | 1 | Min     | 0.98799 | 0.1664  | 0.1644  |
| 2        | 3 | 3 | 3 | Max     | 0.93044 | 1.0     | 0.93044 |
|          | 1 | 1 | 1 | Min     | 0.98797 | 0.17599 | 0.17388 |
| 3        | 3 | 3 | 3 | Max     | 0.93044 | 0.9996  | 0.93011 |
|          | 1 | 1 | 1 | Min     | 0.98802 | 0.17013 | 0.1681  |
| 4        | 4 | 3 | 3 | Max     | 0.9212  | 0.44907 | 0.41368 |
|          | 1 | 1 | 1 | Min     | 0.98802 | 0.082   | 0.08102 |
| 5        | 3 | 3 | 3 | Max     | 0.93044 | 0.44733 | 0.41622 |
|          | 1 | 1 | 1 | Min     | 0.98797 | 0.09213 | 0.09103 |
| 6        | 3 | 4 | 3 | Max     | 0.92123 | 0.45253 | 0.41689 |
|          | 1 | 1 | 1 | Min     | 0.98799 | 0.08947 | 0.08839 |

Due to this characteristic, we can immediately drop the use of joint modules one and two from consideration for use in the configuration. This observation also has a statistical basis as well discussed next. By removing two joint modules from consideration, the joint module combinations under consideration drop from 216 to 64, a 70% reduction in the design space. It is immediately apparent that the RPI, even if a true optimum point cannot be determined, can drastically reduce the design space when trying to determine the configuration for a particular task. Once the design space has been reduced, the configuration can be chosen using additional criteria such as payload, weight, inertia, etc. as was done in Ambrose and Tesar [1].

The locations of the maximum and minimum values from Table 3 are intuitive: the maximum actuator combinations choose the mid-range modules, trading off reliability with precision. It also shows that the RPI is extremely sensitive to the amount of error allowed at the end-effector.

#### 4.3 Significance Studies

Since the data is sorted into four easily identifiable classifications, Analysis of Variance (ANOVA) [14] presents itself as a logical means of studying the differences between the modules and their effect on the Reliability Performance Index. In this case, the factors will be the link options, and the three joint locations: base, elbow and wrist, each with six levels (the different link options and six different joint modules).

There are several different hypothesis tests that can be made using the ANOVA technique. The first is to determine if the effect of a particular factor is a significant contributor to the model. The next test that can be performed is to determine which levels of the different factors are significantly different from the others. Both of these tests are carried out on the data generated from the simulation of the

system of Figure 1 following the trajectory of Figure 2. The data of Figures 3 and 4 were stored on diskette and analyzed using the SAS Statistical Analysis Software System [16].

To study the effects of the joint modules and link options, the interaction effects were added to the error resulting in the ANOVA table of Table 4.

**Table 4. Analysis of Variance Table for the Reliability Performance Index Case Study (Interactions Added to Error)**

| Error Source | Degree of Freedom | Sum of Squares | Mean Square | F*      |
|--------------|-------------------|----------------|-------------|---------|
| B            | 5                 | 20.42          | 4.08        | 729.5   |
| E            | 5                 | 7.8            | 1.56        | 278.97  |
| W            | 5                 | 4.2            | 0.84        | 150.2   |
| L            | 5                 | 41.5           | 8.3         | 1484.01 |
| ERR          | 1275              | 7.131          | 0.00559     |         |
| TOTALS       | 1295              | 81.111         |             |         |

To test for significance of the main effects (B, E, W, and L) we form a null hypothesis of  $H_0$ : Main effects are not significant, which results in the test value  $F_{5, 1275, 0.95} = 2.57$ . Using the rejection region of  $F^* > F$ , we find all of the main effects contribute significantly to the statistical model. We can now test for the significance of the individual levels of the main effects (which was the test we desired). This test is the Tukey Studentized Range test [14, 16]. It determines that a significant difference exists between the means of the effects levels and then makes pairwise comparisons to determine if there is a statistical difference between the two levels. The results of this test is presented in Figures 5 through 8. The brackets under the number lines in Figures 5 through 12 represent statistical differences between the adjacent values on the number line above them. If the bracket overlaps two values, the test could not statistically differentiate between those two values. For instance, in Figure 5, the mean RPI for joint modules 1 and 2 are statistically different since the ranges shown on the brackets underneath do not overlap both module locations on the line. The figure shows that there is no statistical difference between joint modules 6, 5, and 4, but there is a statistical difference between joint modules 6 and 3.

From the examination of Figures 5 through 7, we can see that there is a definite statistical difference in the mean of the RPI when joint modules 1 and 2 are used in any position. The mean value of the RPI is lower for these two joint modules and gives a statistical basis for the conclusion that joint modules 1 and 2 should be removed from the set of possible joint modules. Since there is not any definitive statistical difference between the other joint modules, other design criteria should be used to select the final positions of the joint modules.

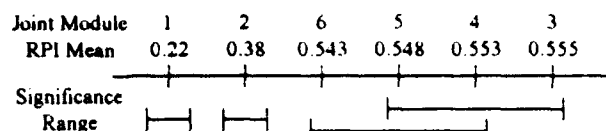


Figure 5. Tukey Studentized Range Test on Levels of Base for the Reliability Performance Index

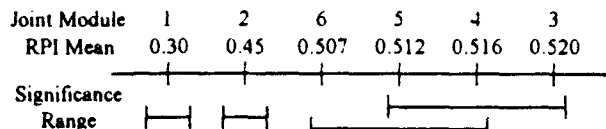


Figure 6. Tukey Studentized Range Test on Levels of Elbow for the Reliability Performance Index

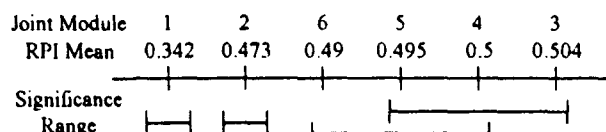


Figure 7. Tukey Studentized Range Test on Levels of Wrist for the Reliability Performance Index

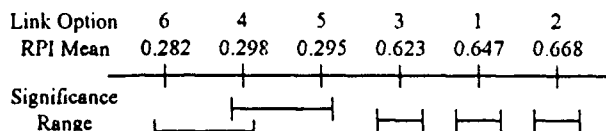


Figure 8. Tukey Studentized Range Test on Levels of Link Option for the Reliability Performance Index

Figure 8 shows the result of the Tukey test for the Link Options. As noted earlier, the difference in length tolerance between the options is significant, however, this test indicates a statistical difference between the first three link options. We can conclude from this test that link option two (which is where the maximum RPI value was located) has a statistically higher mean RPI than the other two tight tolerance link options and should be used. This differentiation does not exist between the wider tolerance suggesting that having large differences between the design levels enables the RPI to better glean the reduced design space for all the design options.

After removing joint modules 1 and 2 from consideration for inclusion into the configuration, the ANOVA and Tukey tests were run again. The removal of the two modules reduced the number of data points to 384 from 1296. Figures 9 through 12 show the results of the Tukey Tests on the reduced data set. The Tukey Tests show that with the reduced data set, we can now see distinct statistical differences between the joint modules RPI means. On the basis of the RPI, we would select joint module 3 for use in all three joint locations. The penalty for the reduction in the data is seen in Figure 12, where we have lost delineation between the link options in each tolerance range. This is

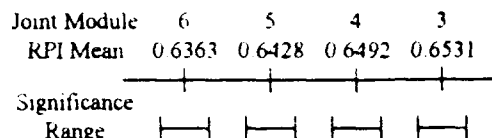


Figure 9. Tukey Studentized Range Test on Levels of Base for the Reliability Performance Index (Reduced Data Set)

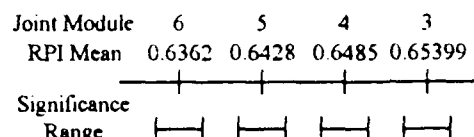


Figure 10. Tukey Studentized Range Test on Levels of Elbow for the Reliability Performance Index (Reduced Set)

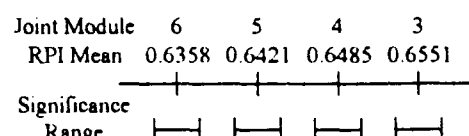


Figure 11. Tukey Studentized Range Test on Levels of Wrist for the Reliability Performance Index (Reduced Set)

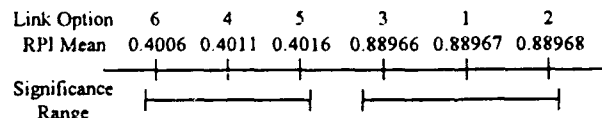


Figure 12. Tukey Studentized Range Test on Levels of Link Option for the Reliability Performance Index (Reduced Set)

correct statistically, since the power of the tests were reduced when data was deleted.

## 5. CONCLUSIONS AND RECOMMENDATIONS

This case study has shown that the framework for the Reliability Performance Index is a useful empirical tool during the selection and design of a configuration of robotic modules of varying reliability and precision. It proves useful as a design guideline to describe how a particular combination or configuration of modules will perform with respect to the system reliability moderated by its precision. While the framework for the RPI was developed, the data to fully investigate its effects on realistic systems is not available.

The RPI does not lend itself to deterministic optimization due to the stochastic nature of the components of the RPI. However, it readily allows for the rejection of module and link combinations as unsuitable, thus reducing the design space. In the case study, analysis of the RPI over the design space suggested that joint modules 1 and 2 could be removed from consideration and that link option 2 presented itself as the best alternative to provide for maximum precision as measured by the RPI. This is a 70% reduction in the joint module design space and an overall

reduction of 95% (by selecting link option 2). Additional tests on a reduced data set (formed by removing joint modules 1 and 2) showed that we could discriminate between the remaining joint modules with the recommendation to use joint module 3 in all joint locations. However, discrimination was lost on the link options since we had much less data to work with.

It was also seen that for larger design spaces and differences in the module characteristics, better discrimination was obtained using the RPI. The use of the RPI allows the designer to eliminate a large portion of the design space and a final design can be selected using other operational design criteria.

Several recommendations concerning the RPI can be made. First, a more thorough investigation of the interactions between the components of the RPI needs to be made. The development of the RPI assumed that while hardware failures will cause a failure in the kinematic sense, the hardware and kinematic reliabilities were independent, which lead directly to the formulation of Equation (1). This is not actually the case, since a failure in the kinematic sense can be dependent upon hardware failures. This dependency should be understood to be able to improve the relationship defined in Equation (1).

The sensitivity of the RPI to the actual design parameters also requires investigation. A way of applying the RPI to monolithic systems may show the same results as to selecting modular configurations, but this requires a direct mapping to design parameters. As shown in [17], a direct relationship exists between the Jacobian of a manipulator and the  $s$ -variances of the end-effector  $s$ -distribution. An analytic formulation is required and will allow the development of the sensitivity of the RPI to the module level design parameters.

The RPI was seen to provide unreliable results when used as a deterministic design optimization criterion. This may not be the case when probabilistic optimization methods are used since the RPI is stochastic in nature. The RPI should be investigated in terms of probabilistic optimizations. Additionally, more realistic examples in the application of the RPI should be developed to determine if the results noted in this small case study can be generally extended.

To take complete advantage of a modular system, the customer requires a way to easily and quickly determine new configurations. The RPI shows promise in reducing the design space for the selection of modular configurations but needs to be incorporated into an on-line computer-aided design system. This will allow the designer to immediately make the indicated configuration or design changes and immediately see the changes in the design criteria, including the RPI.

## 6. ACKNOWLEDGMENTS

This research was supported by the United States Air Force under Educational Services Agreement Number F33600-88-A-0264 and NASA Johnson Space Center Grant Number NAG 9-411 at the University of Texas at Austin.

## REFERENCES

- [1] Ambrose, R. and Tesar, D., "Design, Construction, and Demonstration of Modular Reconfigurable Robots," Research Report, Mechanical Engineering Dept, University of Texas at Austin, Austin TX, August 1991.
- [2] Bhatti, P. and Rao, S., "Reliability Analysis of Robot Manipulators," *Journal of Mechanisms, Transmissions, and Automation in Design*, v.110, June 1988, pp. 175-181.
- [3] Butler, M. and Tesar, D., "An Applications-Based Assessment of Present and Future Robot Development," Research Report, Department of Mechanical Engineering, University of Texas at Austin, Austin, TX, May 1992.
- [4] Craig, J., *Introduction to Robotics Mechanics and Control*, Addison-Wesley, New York, 1989.
- [5] Denavit, J. and Hartenberg, R., "A Kinematic Notation for Lower-Pair Mechanisms Based on Matrices," *ASME Journal of Applied Mechanics*, June 1955, pp. 215-221.
- [6] Ireson, W. and Coombs, C., Jr. (eds.), *Handbook of Reliability Engineering and Management*, McGraw-Hill, New York, 1988.
- [7] Kapur, K. and Lamberson, L., *Reliability in Engineering Design*, John Wiley, New York, 1977.
- [8] Kubat, P., "Assessing Reliability of Modular Software," *Operation Research Letters*, v. 8, n.1, Feb 1989, pp. 35-41.
- [9] Littlewood, B., "Software Reliability Model for Modular Program Structure," *IEEE Transactions on Reliability*, v. 28, n. 3, Aug 1979, pp. 241-246.
- [10] Lovett, J. and Tesar, D., "Task Requirements for Robotic Maintenance Systems for Nuclear Power Plants," Research Report, Department of Mechanical Engineering, University of Texas at Austin, Austin, TX, August 1989.
- [11] McAndrew, D. and Tesar, D., "Assessment of Microelectronics Assembly in Terms of the Development of Precision Layered Control Mechanisms," Research Report, Mechanical Engineering Dept, University of Texas at Austin, Austin, TX, Dec 1991.
- [12] Mendenhall, W., Schaeffer, R., and Wackerly, D., *Mathematical Statistics with Applications*, Duxbury Press, Boston, MA, 1981.
- [13] Mooring, B. and Pack, T., "Aspects of Robot Repeatability," *Robotica*, v. 5, pt. 3, Jul/Sept 1987, pp. 223-230.
- [14] Neter, J., Wasserman, W., and Kutner, M., *Applied Linear Statistical Models*, 3rd ed., Richard D. Irwin, Inc., Homewood, IL, 1990.
- [15] Ross, S., *Introduction to Probability Models*, Academic Press, New York, 1989.
- [16] SAS/STAT User's Guide, Release 6.03, SAS Institute, Cary, NC, 1988.
- [17] Schneider, D., "Reliability and Maintainability of Modular Robot Systems: A Roadmap for Design," Dissertation, Department of Mechanical Engineering, University of Texas at Austin, Austin, TX, August 1993.



## BIOGRAPHIES

Dean L. Schneider, Ph.D.  
Captain, USAF  
AFIT/ENG  
2950 P. Street  
Wright-Patterson AFB, OH 45433-7765

Captain Schneider was commissioned on 7 May 1982 after receiving his BSEE at Texas A&M University. He was assigned to the 381 Strategic Missile Wing, McConnell AFB, Wichita, Kansas, where he was responsible for on-site engineering problems until 1985. After completing a MSEE in digital control theory at the Air Force Institute of Technology in 1987, he was assigned to the San Antonio Air Logistic Center, Kelly AFB, San Antonio, Texas as a reliability engineer responsible for the depot Environmental Stress Screening and Electrostatic Discharge Control Programs. In 1989 he was re-assigned as the assistant to the SA-ALC Chief Scientist assisting in the development of engineering and scientific policy and technical personnel management issues. He was selected to attend a doctoral program in 1990 and subsequently was assigned to the faculty of the Air Force Institute of Technology in 1993. Captain Schneider has been awarded the Air Force Commendation and Meritorious Service Medals and was the AFLC Outstanding Company Grade Military Engineer of 1989 and the 1989 SA-ALC Company Grade Officer of the Year. Captain Schneider is a member of the IEEE, Eta Kappa Nu, the IEEE Reliability and Control Systems Societies, and the Air Force Association.

Delbert Tesar, Ph.D., P.E.  
University of Texas at Austin  
BRC/MERB  
Mail Code # 79925  
Austin, Texas, 78712-1100

Professor Tesar holds the Carol Cockrell Curran Chair in Engineering at the University of Texas at Austin and is Director of the University of Texas Robotics Research Group. Dr. Tesar supervises over 30 graduate students covering topics in modular robotic system design, automated robotic system design, robotic system fault tolerance, actuation, and robot control. The program is funded at \$2 million dollars and occupies 16,000 square feet of laboratory space at the University of Texas Balcones Research Center. Dr. Tesar received his Ph.D. in Mechanical Engineering from the Georgia Institute of Technology in 1964 and has authored 132 reviewed technical papers, 52 position papers, and has formulated 89 major research reports. He has supervised 62 Masters Theses and 28 Doctoral Dissertations. Dr. Tesar is the author (with G. K. Matthew) of a reference book *Modeled Cam Systems - Analysis, Design, and Synthesis*, Lexington Books, 1976, dealing with the design of precision machines operating at high speeds.

J Wesley Barnes, Ph.D., P.E.  
University of Texas at Austin  
ETC 5.128B  
Mail Code # 62200  
Austin, Texas, 78712

Professor Barnes is a Professor of Mechanical Engineering and the Cullen Trust for Higher Education Endowed Professor in Engineering No. 6 at the University of Texas at Austin. Prior to joining the University of Texas in 1974, he was employed by Tracor Inc. and Bell Telephone Laboratories. He is a past Associate Editor of the *Transactions of the Institute of Industrial Engineers* and is a Registered Professional Engineer in the State of Texas. He is very active in graduate research and supervision and possesses extensive industrial and consulting experience. He is the author of several books, among them are *Network Flow Programming*, Winner of the Institute of Industrial Engineers Book-of-the-Month Award for 1980 and *Statistical Analysis for Engineers. A Computer Based Approach, Revised Edition*, McGraw-Hill Publishing Co., forthcoming in 1994.

| REPORT DOCUMENTATION PAGE   |   |  | Form Approved<br>OMB No 0704-0188                                   |   |
|---|---|--|---|---|
| <small>Public reporting burden for this collection of information is estimated to average 1 hour per response, including the time for reviewing instructions, searching existing data sources, gathering and maintaining the data needed, and completing and reviewing the collection of information. Send comments regarding this burden estimate or any other aspect of this collection of information, including suggestions for reducing this burden, to Washington Headquarters Services, Directorate for Information Operations and Reports, 1215 Jefferson Davis Highway, Suite 1204, Arlington, VA 22202-4302, and to the Office of Management and Budget, Paperwork Reduction Project (0704-0188), Washington, DC 20503.</small>   |   |  |   |   |
| 1. AGENCY USE ONLY (Leave blank)  |   | 2. REPORT DATE<br>Oct 93                                 |   | 3. REPORT TYPE AND DATES COVERED<br>Final |
| 4. TITLE AND SUBTITLE<br>Development & Testing of a Reliability Performance Index for Modular Robotic Systems   |   |  | 5. FUNDING NUMBERS  |   |
| 6. AUTHOR(S)<br>Schneider, D., Tesar, D., and Barnes, J.  |   |  |   |   |
| 7. PERFORMING ORGANIZATION NAME(S) AND ADDRESS(ES)<br>Air Force Institute of Technology, AFIT/ENG<br>Wright-Patterson AFB, OH 45433<br><br>The University of Texas at Austin, Mech. Engr. Dept<br>Stop 79925, Austin, TX 78712  |   |  | 8. PERFORMING ORGANIZATION<br>REPORT NUMBER<br><br>AFIT/EN/TR-93-08 |   |
| 9. SPONSORING / MONITORING AGENCY NAME(S) AND ADDRESS(ES)   |   |  | 10. SPONSORING / MONITORING<br>AGENCY REPORT NUMBER                 |   |
| 11. SUPPLEMENTARY NOTES<br>To be published in the proceedings of the 1994 Annual Reliability and Maintainability Symposium, Anaheim, CA, 24-28 Jan 1994.  |   |  |   |   |
| 12a. DISTRIBUTION / AVAILABILITY STATEMENT<br><br>Approved for public release: Distribution Unlimited   |   |  | 12b. DISTRIBUTION CODE  |   |
| 13. ABSTRACT (Maximum 200 words)<br><br>Using a probabilistic representation of manipulator kinematics and a reliability block diagram model of the manipulator system, a Reliability Performance Index (RPI) representing the probability of no hardware or software failure and the manipulator achieving a specified position and orientation is developed. The RPI is tested with a case study consisting of a three degree-of-freedom planar manipulator assembled from a choice of six joint modules of varying reliability and precision and a choice of six link module combinations of varying lengths and machining tolerances. A straight-line, square trajectory is specified and the RPI is calculated for each combination of joint modules and links, a total of 1296 different combinations. Using statistical testing, a 70% reduction in the module design space is achieved using the RPI. Optimization using other appropriate manipulator criteria can then be performed to generate the final configuration. Additional extensive case studies are needed to fully develop the RPI to a stage necessary for implementation into a computer-aided design system for modular robot configuration design. The RPI may also be useful in the quantification of the overall system reliability and performance of any system based upon measured error, such as control systems. |   |  |   |   |
| 14. SUBJECT TERMS<br>Modular Robotic Systems, Reliability Index, Kinematic Reliability, Accuracy  |   |  | 15. NUMBER OF PAGES<br>9  |   |
|   |   |  | 16. PRICE CODE  |   |
| 17. SECURITY CLASSIFICATION<br>OF REPORT<br><br>UNCLAS  | 18. SECURITY CLASSIFICATION<br>OF THIS PAGE<br><br>UNCLAS | 19. SECURITY CLASSIFICATION<br>OF ABSTRACT<br><br>UNCLAS | 20. LIMITATION OF ABSTRACT<br><br>UL                                |   |